

NEW RESULTS ON CHARMED D , F^\pm AND F^* PRODUCTION AND DECAY FROM THE MARK III†

RAFE H. SCHINDLER representing The MARK III Collaboration

Stanford Linear Accelerator Center
 Stanford University, Stanford, California 94305

Results on charmed meson production and decay are presented from the Mark III at SPEAR. $F\bar{F}^*$ associated production is observed allowing a direct measurement of the F^* mass. A search for the decay $D^+ \rightarrow \mu^+ \nu_\mu$ in the recoil of hadronically tagged D^\pm decays provides a stringent limit on the pseudoscalar decay constant f_D . New results on $D^0\bar{D}^0$ mixing from semileptonic D^0 decays and evidence for a nonresonant component in D_{e4} decays are also presented.

1. $F\bar{F}^*$ ASSOCIATED PRODUCTION

Evidence for the charmed vector meson F^* has been previously reported.¹ Interest lies in a precise mass determination providing a strict test of the constancy of the pseudoscalar-vector mass² splitting predicted by Frank and O'Donnell.²

In a sample of $6.3 \pm 0.5 \text{ pb}^{-1}$ integrated luminosity taken at $\sqrt{s} = 4.14 \text{ GeV}/c^2$, a search is performed for \bar{F}^* produced in association with an $F^+ \rightarrow \phi\pi p$. Charged tracks in the analysis are constrained to the beam position and a common event vertex. Charged kaons are identified by time-of-flight. The invariant mass of all K^+K^- pairs is formed and those lying within $\pm 0.010 \text{ GeV}/c^2$ of the ϕ mass are combined with all other tracks in an event which are assumed to be pions. The recoil mass of each $\phi\pi$ combination is calculated and displayed in Fig. 1. Events appear to cluster in the recoil of the $\phi\pi$ when it is near either the D^\pm or

the F mass. Cutting on recoil masses from 1.97 to 2.05 GeV and 2.05 to 2.15 provides clean signals for both the Cabibbo suppressed D^\pm decay and the F , respectively (see Fig. 2). There are 9 D^\pm signal events and $29.4 \pm 5.4 F^\pm$ events. The backgrounds are determined from event mixing. The F^\pm mass is found to be $1.9734 \pm 0.0044 \pm 0.0040 \text{ GeV}/c^2$.

The cluster of events recoiling from $F \rightarrow \phi\pi$ is expected to be a compound distribution. From Fig. 1, most events appear to originate from $F\bar{F}^*$ production, there being little evidence for $F\bar{F}$ production. The $\phi\pi$ events at the F mass can arise either from the direct F or from the decay of the $\bar{F}^* \rightarrow \gamma + \phi\pi$. To improve the F^* mass resolution a simple kinematic constraint is applied. The observed $F \rightarrow \phi\pi$ is assumed to be a direct F , and its mass is fixed at $1.9705 \text{ GeV}/c^2$.

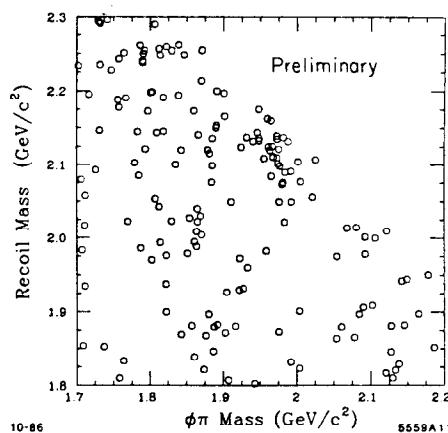


Figure 1: $\phi\pi$ mass vs recoil mass.

†Work supported in part by the Department of Energy, under contracts DE-AC03-76SF00515, DE-AC02-76ER01195, DE-AC03-81ER40050, and DE-AM03-76SF00034.

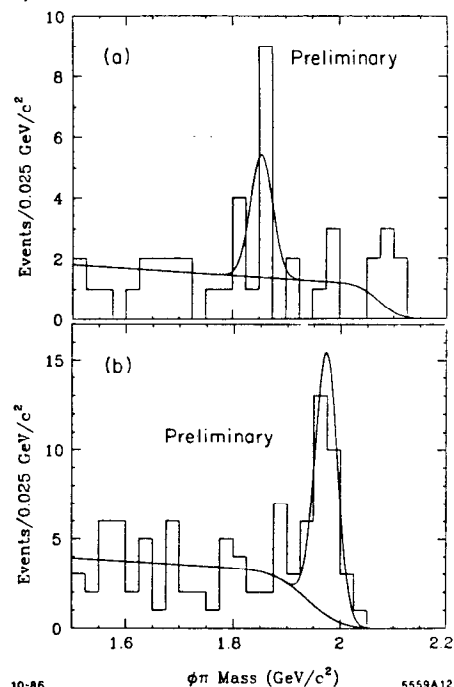


Figure 2: $\phi\pi$ mass for recoil cuts emphasizing $D\bar{D}^*$ and $F\bar{F}^*$ production.

The invariant mass of the F^* is then calculated assuming that its energy is that of the beam, less that of the detected $\phi\pi$. This should result in a $0.005 \text{ GeV}/c^2$ mass resolution when the $\phi\pi$ is direct, and a wider ramp-like distribution if it is from the F^* . The $\phi\pi$ are expected to populate both distributions equally. The results are shown in Fig. 3. The mass of the F^* is $2.1108 \pm 0.0019 \pm 0.0032 \text{ GeV}/c^2$. The systematic error includes uncertainties in both the detector mass scale, as well as the beam energy. Since the F^* mass is not independent of the F mass, the $F-F^*$ mass splitting is best obtained taking a world average³ (1.9705 ± 0.0025) for the F mass that excludes our measurement. The resulting mass difference is $0.137 \pm 0.007 \text{ GeV}/c^2$. This implies a difference in squared masses for the F and F^* of 0.56 ± 0.03 in good agreement with the lighter mesons, as predicted by Frank and O'Donnell,² and implying that the mesonic wavefunction at the origin for a meson containing both heavy and light quarks is largely determined by the long range confining part of the interquark potential.

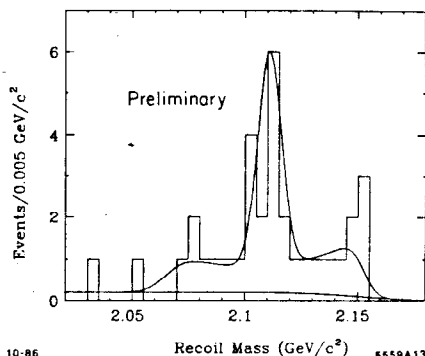


Figure 3: F^* mass assuming $F\bar{F}^*$ production.

The observed events, after correction for detection efficiency (0.063), yield a value of $\sigma(e^+e^- \rightarrow F\bar{F}^*) \cdot Br(F \rightarrow \phi\pi) = 36 \pm 7 \pm 13 \text{ pb}$ for the production rate.

2. THE PSEUDOSCALAR DECAY CONSTANT (f_D)

The D meson decay constant (f_D) is a physical quantity of great theoretical interest. The constant f_D may be unambiguously measured through the pure leptonic decay of the D^\pm :

$$\Gamma_{D^+ \rightarrow \mu^+ \nu} = \frac{G_F^2}{8\pi} f_D^2 m_D m_\mu^2 |V_{cd}|^2 \times (1 - (m_\mu/m_D)^2)^2$$

The decay constant is a direct measure of the overlap of the wavefunctions of the heavy and light quarks in the D meson.⁴ It thus plays a fundamental role in setting the scale for processes such as weak flavor annihilation and Pauli interference invoked to account for the differences in D^\pm and D^0 lifetimes.⁵ A measurement of f_D also provides a stringent test

of potential model⁴ and QCD sum rule⁶ calculations. In addition, it allows reliable estimates of other heavy meson decay constants ($f_F, f_B, \text{etc.}$), which are difficult to obtain due to the large theoretical uncertainties in extrapolating from f_π and f_K to the nonrelativistic heavy quark mesons. The decay constant also is essential in evaluating the magnitude of operators leading to $D^0\bar{D}^0$ and $B^0\bar{B}^0$ mixing.⁷

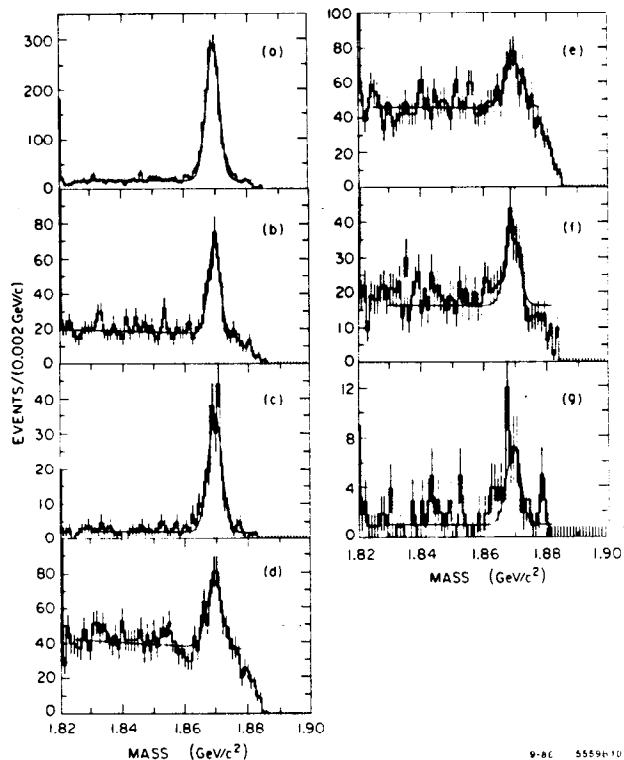


Figure 4: Shown are the mass plots for the seven D^\pm tags used in this analysis: (a) $K^-\pi^+\pi^+$, (b) $\bar{K}^0\pi^+\pi^+\pi^-$, (c) $\bar{K}^0\pi^+$, (d) $\bar{K}^0\pi^+\pi^0$, (e) $\bar{K}^-\pi^+\pi^+\pi^0$, (f) $K^-K^-\pi^+$, and (g) \bar{K}^0K^+ .

The data employed (9.3 pb^{-1}) were obtained at $\sqrt{s} = 3.768 \text{ GeV}$, where charmed D mesons are produced only in pairs. The search is carried out by isolating a sample of events in which a D^+ candidate is found, and then examining the recoil system for evidence of the $\mu^-\nu_\mu$ decay. Seven hadronic D^\pm tags are used: $K^-\pi^+\pi^+$, $\bar{K}^0\pi^+$, $\bar{K}^0\pi^+\pi^+\pi^-$, $\bar{K}^0\pi^+\pi^0$, $\bar{K}^-\pi^+\pi^+\pi^0$, \bar{K}^0K^+ , and

$K^-K^+\pi^+$, resulting in 2490 ± 42 (stat) ± 40 (syst) cleanly identified D^\pm (see Fig. 4).

The isolation of the $\mu^- \bar{\nu}_\mu$ candidates proceeds by requiring the recoil system from a tag to have one track with a charge opposite to that of the tag whose momentum must lie between 0.775 and 1.125 GeV/c. The event must be consistent with having zero missing mass,² when the track is assigned a muon mass. Monte Carlo distributions for the expected signal are shown in Fig. 5. After the momentum cut, missing mass² is required to lie between -0.265 and 0.175 $(\text{GeV}/c^2)^2$ losing about 5% of the expected signal.

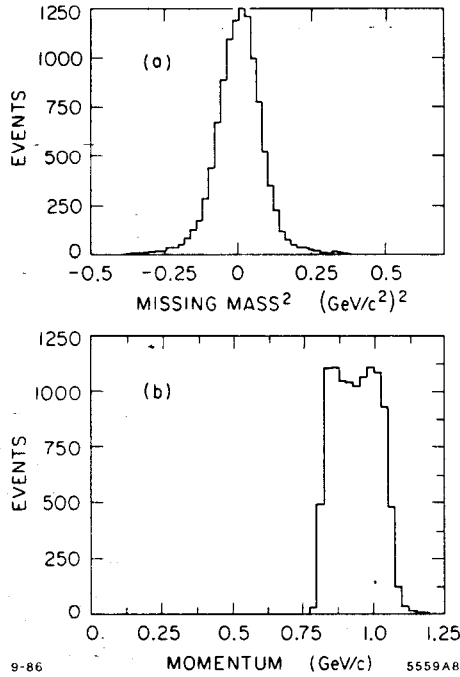


Figure 5: Monte Carlo showing (a) the missing mass² and (b) the expected momentum distribution, for $D^+ \rightarrow \mu^+ \nu_\mu$.

Muon candidates must either lie in the acceptance of the muon system ($|\cos\theta| \leq 0.65$) or lie where there is calorimetric information. Tracks entering the muon system must have two (one) layer hit for muon momentum ($p_\mu \geq 1$ GeV/c ($p_\mu < 1$ GeV/c)). No other topological cuts are applied due to the (90 - 95%) rejection of π and K decays and punchthrough provided by the muon system.⁸

If the muon candidate lies outside the muon system it is required to be minimum ionizing in the calorimeter (≤ 0.300 GeV deposited). Additional cuts on these events are imposed to reduce the principle sources of background from the decays $D^+ \rightarrow \bar{K}^0 \pi^+$, $\pi^+ \pi^0$, $\bar{K}^0 K^+$, and $\bar{K}^0 \mu^+ \nu$. Background events with a π^0 (either from the D^- or a

$K_S^0 \rightarrow \pi^0 \pi^0$) are rejected by requiring the absence of any isolated photons in an event (isolated photons are defined as those not used in forming a π^0 in the tag, or which make an angle $|\cos\theta| \leq 0.92$ with respect to any charged track). This cut also rejects K_L^0 interacting in the shower counter. The fraction of K_L^0 which interact is modeled by using the decay $\psi(3100) \rightarrow K_S^0 K_L^0$, $K_S^0 \rightarrow \pi^+ \pi^-$ from a separate data set.⁹ Due to the larger cross-section for K_L^0 at the momentum found in the $\psi(3100)$ data, this procedure is expected to underestimate the background.

The expected missing mass squared (M_{miss}^2) is zero for $D^- \rightarrow \mu^- \bar{\nu}_\mu$, while it is expected to peak near $m_{\pi^0}^2$ or $m_{K_S^0}^2$ for the two body backgrounds. In the case of $\bar{K}^0 \mu^- \bar{\nu}_\mu$, the missing ν_μ makes M_{miss}^2 peak above $m_{K_S^0}^2$ (see Fig. 6).

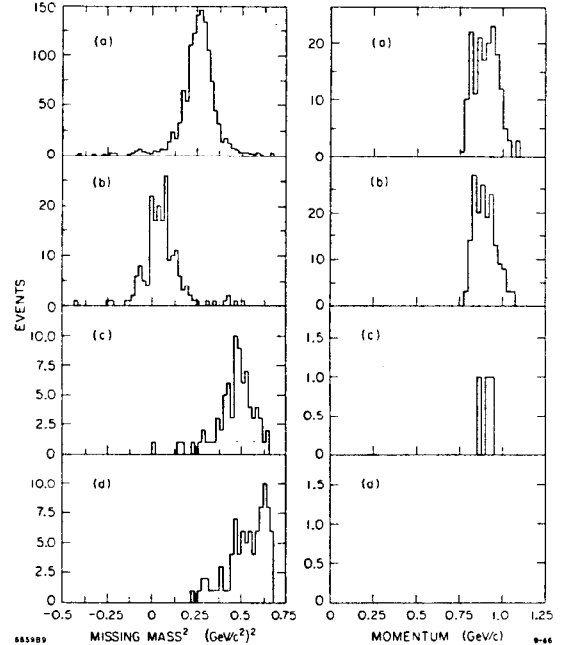


Figure 6: The variables M_{miss}^2 and p_μ^{ab} are plotted for Monte Carlo events for the four major backgrounds: (a) $D^+ \rightarrow \bar{K}^0 \pi^+$, (b) $\pi^+ \pi^0$, (c) $\bar{K}^0 K^+$, and (d) $\bar{K}^0 \mu^+ \nu$. The variables M_{miss}^2 and p_μ^{ab} are plotted for Monte Carlo events for the four major backgrounds: (a) $D^+ \rightarrow \bar{K}^0 \pi^+$, (b) $\pi^+ \pi^0$, (c) $\bar{K}^0 K^+$, and (d) $\bar{K}^0 \mu^+ \nu$.

When these cuts are applied to the data, no events are found to survive (Fig. 7). The nearest event to the M_{miss}^2 cut appears lies 20 $(\text{MeV}/c^2)^2$ at 0.196 $(\text{GeV}/c^2)^2$.

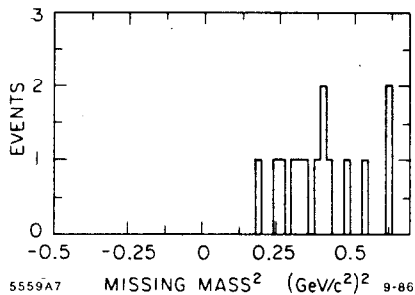


Figure 7: Missing mass² for data, after P_{μ}^{lab} cut.

The expected background with these cuts is 1.16 ± 0.16 (stat.) ± 0.20 (syst.) The error from the underestimate of the background component containing a K_L^0 is excluded from the systematic error because of the uncertainty in the size of the effect. The background calculation is tested by loosening the muon selection criteria, and comparing the number of events observed to that predicted by the Monte Carlo. Removing all muon identification 12 events are accepted within the kinematic cuts as compared to a prediction of 5.8 from the four charmed meson sources described. A further check is made using the observed M_{miss}^2 distribution. Events from $D^+ \rightarrow \bar{K}^0 \mu^+ \nu_{\mu}$ and $D^+ \rightarrow \bar{K}^0 \pi^+$ are expected to have M_{miss}^2 larger than $m_{K^0}^2$. Ten events are observed in the data from 0.2 to 0.5 (GeV/c²)². This is consistent with 7.6 events predicted by the Monte Carlo for charmed backgrounds, thus providing additional experimental verification for the estimate.

The observation of no events of the type $D^+ \rightarrow \mu^+ \nu_{\mu}$ together with the background prediction yields a 90 % Confidence Level (C.L.) upper limit of 1.35 signal events.¹⁰ The probability of observing no events when 1.0 background events are expected is 0.37. The acceptance for this decay mode varies by less than 3% for the seven different tagging modes; a weighted average of $0.72 \pm .01$ (stat) $\pm .05$ (syst) is used. Dividing by the acceptance and the total number of D^{\pm} tags¹¹ gives a 90% C.L. upper limit on the branching ratio of 8.4×10^{-4} . Using a D^{\pm} lifetime of $(10.1^{+0.7}_{-0.6}) \times 10^{-13}$ s,¹² and $|V_{cd}|^2 = 0.0506 \pm .0065$ ¹³ then the 90 % C.L. branching ratio limit corresponds to $f_D = 310$ MeV/c². When the errors on τ_{D^+} and $|V_{cd}|^2$ are included, we obtain a 90 % C.L. upper limit on f_D of 340 MeV/c², (see Fig. 8).

Calculations of the pseudoscalar decay constants obtain values which either increase (QCD sum rule method⁶) or decrease (non-relativistic potential⁴ and bag model methods¹⁴ with the meson mass. While our result does not probe the small values of f_D suggested by the bag model or QCD sum

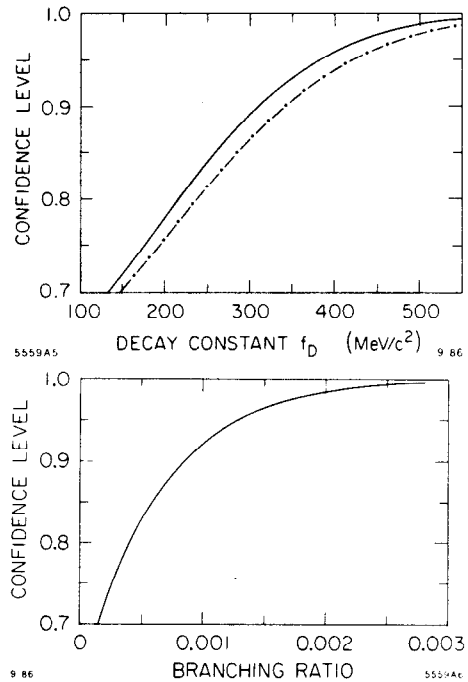


Figure 8: Shown is the Confidence Level (C.L.) for our result as a function of (a) $B(D^+ \rightarrow \mu^+ \nu_{\mu})$, and (b) f_D . The limit calculation is described in reference (10). The dashed curve in (b) includes the effects of lowering the values of τ_{D^+} and $|V_{cd}|^2$ by their errors.

rule calculations (150 \rightarrow 280 MeV/c), it restricts the range of values predicted by recent potential model calculations (208 \rightarrow 450 MeV/c). It also excludes the very high values of f_D which have been suggested¹⁵ as an explanation for the large observed ratio of $\tau(D^+)/\tau(D^0)$.

3. $D^0 \bar{D}^0$ MIXING

Previously,¹⁶ we have reported results of a search for $D^0 \bar{D}^0$ mixing candidates carried out by examining $D^0 \bar{D}^0$ events having strangeness of ± 2 , when the D^0 (or \bar{D}^0) decayed hadronically to either $K^- \pi^+$, $K^- \pi^+ \pi^+ \pi^-$ or $K^- \pi^+ \pi^0$ (or charge conjugates). This results in the observation of three $s = \pm 2$ events with an estimated background of $0.4 \pm 0.1 \pm 0.1$ from particle misidentification. The sample also includes 162 fully reconstructed events where $s = 0$. Because these $D^0 \bar{D}^0$ events decay to hadronic final states, a background from doubly Cabibbo suppressed decays (DCSD) may be present.¹⁷ This background is only absent in the case of identical final states. To reduce or eliminate the problem of DCSD the search has been extended to fully reconstructed events containing either a hadronic plus a semileptonic decay ($K^- e^+ \nu$ or $K^- \mu^+ \nu$), or two semileptonic decays, respectively.

The semileptonic sample is selected requiring a hadronic tag where $\delta \geq 150\text{ps}$ or $\delta \geq 1\sigma$ for time-of-flight (TOF) or DEDX identification, respectively. Here δ is the maximum value for the difference of the observed time of a π or K in $K^-\pi^+$ or $K^-\pi^+\pi^0$ decays from the average expected time for a π or K hypothesis. In the $K^-\pi^+\pi^+\pi^-$ mode, δ is tested for the K^- only. Recoiling from the hadronic tag, we demand there be no isolated photons in candidate events. The recoil semileptonic decay requires a loosely identified K^\pm ($\delta \geq 100\text{ps}$ TOF or 1σ DEDX) and an identified lepton (e or μ). Monte Carlo studies indicate that hadronic versus hadronic events can leak into the semileptonic versus hadronic classification if a hadron is misidentified as a lepton. These decays would peak near zero missing transverse momentum (p_T^{miss}) in the event. Additional p_T^{miss} can arise from asymmetric π^0 's that escaped the cut on additional isolated photons. Figure 9 shows the p_T^{miss} distributions for backgrounds, the expected signal, and the data. A cut at $p_T^{\text{miss}} \geq 0.150 \text{ GeV}/c$ is made retaining 74 events. The expected background is 5 events leaving 69 mixing candidates. All these events are found to be *correct sign*; the charge of the lepton being opposite to that of the kaon in the tag.

Semileptonic versus semileptonic events are analyzed by selecting four prong events with zero

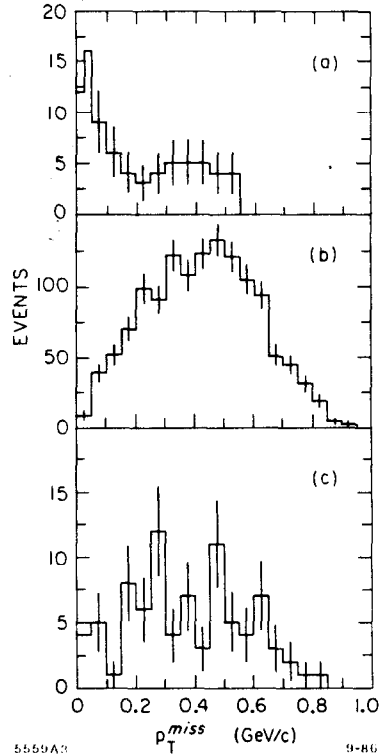


Figure 9: (a) p_T^{miss} for hadronic backgrounds. (b) for semileptonic decays. (c) for data.

net charge, and no isolated photons. Here we require *either* a solid tag on strangeness (2 well identified K^\pm and ≥ 1 lepton), or a solid tag on the 2 leptons ($\geq 1K^\pm$ and 2 identified leptons). At least one combination must be consistent with the monochromatic pair production of $K^1l^1\nu^1$ versus $K^2l^2\nu^2$. That is, the momentum of each neutrino ($p_\nu^i, i = 1, 2$) must satisfy:

$$p_\nu^i = 1.884 - E(K^i + l^i) \geq 0.$$

$$|p_\nu^i - P(K^i + l^i)| \leq 283 \text{ MeV}/c$$

$$p_\nu^i + P(K^i + l^i) \geq 283 \text{ MeV}/c$$

The resulting distribution for the ν^i energy is shown in Fig. 10 for Monte Carlo and data. The data shows evidence for a low energy tail which comes from semileptonic versus hadronic events, where the latter has a lepton misidentification. There is also evidence for a high energy tail which may result from the loss of a neutral hadron (K_L^0) in a semileptonic versus hadronic event, as well as a lepton misidentification. To reduce these backgrounds, the cuts in this preliminary analysis are tightened requiring both leptons and both kaons to be well identified. This introduces a large inefficiency as is evidenced in Fig. 11. The result is 12 events, *all* found to contain opposite signed leptons.

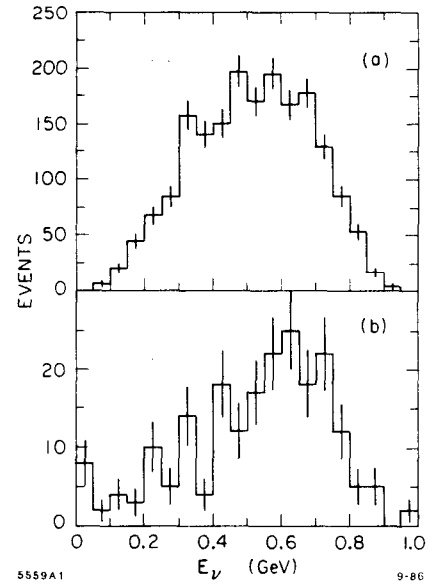


Figure 10: Neutrino energy for (a) Monte Carlo and (b) data.

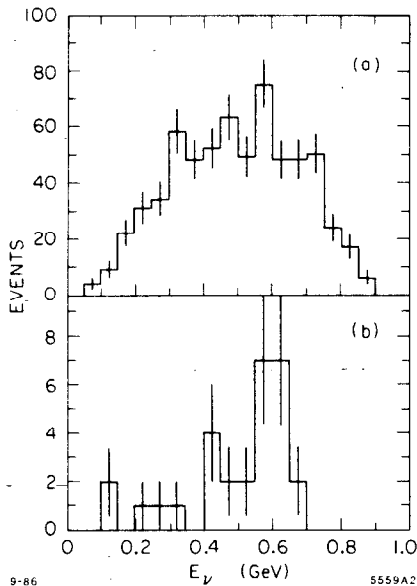


Figure 11: Neutrino energy for (a) Monte Carlo and (b) data, after tightened cuts.

To interpret our preliminary results, we considered the data under two extreme cases. First we assume that there is no contribution from DCSD. In the language of Bigi and Sanda¹⁷ the parameter $\rho = 0$. In this case, we would "explain" the excess $s = \pm 2$ events as originating from $D^0 \bar{D}^0$ mixing, and arrive at a mixing parameter $r \approx 0.01$ with an error of 60%. This would be unexpected large since even long range effects produce values for r typically less than 0.002.¹⁷ The excess events may alternately be attributed to the presence of DCSD. We then determine a minimum value for $\rho^2 \approx 5 \tan^4(\theta_c)$ with a similar error. This value is also surprisingly large (see Bigi and Sanda) but must be considered in conjunction with its error derived from three events.

4. EVIDENCE FOR A NONRESONANT D_{e4} DECAYS

Previously,¹⁹ we have reported the exclusive reconstruction of semileptonic D_{e3} and D_{e4} decays opposite hadronic tags. The analysis is similar to that used in the mixing analysis. In the decays to $K^-\pi^+ e^+\nu$, $\bar{K}^0\pi^- e^+\nu$ and $\bar{K}^-\pi^0 e^+\nu$ it is possible to examine the $K\pi$ subsystem for resonant structure. Figure 12 shows the invariant mass for D_{e4} decays from 39 reconstructed events. The expected background in this plot is about one event. While the plot shows evidence for a strong $K^*(892)$ signal, there are excess events below and above the peak. The entire distribution has been fit to a superposition of $K^*(892)$ and $K\pi$ phase space in an s-wave. The results have been overplotted in the figure. Fitting for the two channels, we determine the fraction of s-wave²⁰ to be $45^{+14}_{-13}\%$ (stat. errors only). This

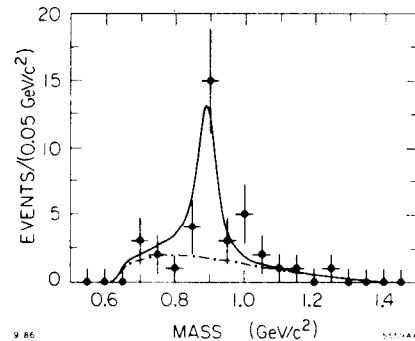


Figure 12: $K\pi$ invariant mass for D_{e4} decays. The curve is described in the text.

result agrees well with the average of the two fits of the DELCO measurement of the inclusive spectrum of leptons from charm decays.²¹

Interestingly, no models of charm semileptonic decay have treated the case of a large non-resonant component. The value obtained implies that approximately 1/4 of all semileptonic decays occur non-resonantly. This is similar to the nonresonant fraction of the hadronic sector.²²

5. CONCLUSIONS

We have presented evidence for the associated production of the pseudoscalar F meson and its vector partner, allowing a precise mass determination. A limit on the pseudoscalar decay constant of the D has been established. We have extended the search for $D^0 \bar{D}^0$ mixing to the semileptonic sector, finding no additional candidates. Evidence for a nonresonant component to the D_{e4} decays has been presented.

REFERENCES

1. H. Albrecht *et al.*, Phys. Lett. **146B**, 111 (1984), H. Aihara *et al.*, Phys. Rev. Lett. **53**, 2465 (1984).
2. M. Frank and P. O'Donnell, Phys. Lett. **159B**, 174 (1985)
3. M. Aguilar-Benitez *et al.*, Phys. Lett. **170B**, (1986).
4. S. N. Sinha, Alberta THY-3-86 (1986); P. J. O'Donnell, CERN-TH-4419/86 (1986); L. Maiani, Proc. of XXI Int. Conf. on High Energy Physics, (Editions de Physique, Le Ulis, France, 1982), pp. 631-657; H. Krasemann, Phys. Lett. **96B**, 397 (1980).
5. R. M. Baltrusaitis, *et al.*, Phys. Rev. Lett. **54**, 1976 (1985).
6. V. S. Mathur and M. T. Yamawaki, Phys. Rev. **D29**, 2057 (1984); V. A. Novikov, *et al.*, Phys. Rev. Lett. **38**, 626 (1977).

7. I. I. Bigi, G. Köpp, and P. M. Zerwas, *Phys. Lett.* **166B**, 238 (1986); J. F. Donoghue, *et al.*, *Phys. Rev.* **D33**, 197 (1986).
8. R.M. Baltrusaitis, *et al.*, *Phys. Rev. Lett.* **55**, 1842 (1985).
9. R.M. Baltrusaitis, *et al.*, *Phys. Rev.* **D55**, 566 (1985).
10. The C.L. is defined as the probability that a given hypothesis (here, the sum of the signal (n_s) and background (n_b)) will give an observed number of events that is greater than the number actually seen by the experiment. The probability of an experimental result is the joint probability of two Poisson distributions (for n_s and n_b). See M. Aguilar-Benitez *et al.*, *Rev. Mod. Phys.* **56**, S46 (1984), A. G. Frodesen *et al.*, *Probability and Statistics in Particle Physics (Universitetsforlaget, Bergen, 1979)*, pp. 167-168, 378-379. Thus, the limit on n_s at the 90% C.L. is derived from the limit on ($n_s + n_b$) by subtraction of n_b from 2.3 events. The statistical error on n_b is incorporated by fluctuating n_b in the Poisson with a Gaussian distribution, while the systematic error is directly subtracted from the central value of n_b , to provide a more conservative limit. This gives 1.35 events as the 90% C.L. limit. Alternately, if an *a priori* uniform distribution of signal events is assumed, then the 90% C.L. upper limit on n_s would be 2.3 events.
11. The errors on the number of tags and the acceptance are subtracted in order to give a more conservative limit. We thus use .662 for the acceptance, and 2408 as the number of tags.
12. V. Lüth, *Proc. of Int. Symposium on Production and Decay of Heavy Flavors, Heidelberg, May 20-23, 1986*, to be published.
13. M. Aguilar-Benitez *et al.*, *Rev. Mod. Phys.* **56**, S43 (1984).
14. E. Golowich, *Phys. Lett.* **91B**, 271 (1980), M. Claudson, HUTP-81/A016 (1982).
15. M. Bander, D. Silverman, A. Soni, *Phys. Rev. Lett.* **44**, 7 (1980).
16. G. Gladding, *5th Int. Conf. on Physics in Collision, Autun, France July 2-5, 1985*.
17. I. Bigi, A. Sanda, *Phys. Lett.* **171B**, 320 (1986).
18. See for example J. Donoghue *et al.*, *Phys. Rev.* **D33**, 179 (1986) and references therein.
19. D. Coffman, *Proc. of the XXI Rencontre de Moriond, March 1986*, to be published.
20. A p -wave fit was also tried, resulting in a slightly poorer fit.
21. W. Bacino *et al.*, *Phys. Rev. Lett.* **43**, 1073 (1979). Here $37 \pm 16\%$ and $55 \pm 21\%$ were obtained assuming pure K^* and pure non-resonant $K\pi$, respectively.
22. See for example, R. H. Schindler, *Proc. of the SLAC Summer Institute on Particle Physics, (1985)*.